

Reinhard Windoffer · Bernhard Beile · Antje Leibold  
Sabine Thomas · Ursula Wilhelm · Rudolf E. Leube

## Visualization of gap junction mobility in living cells

Received: 6 September 1999 / Accepted: 16 November 1999 / Published online: 3 February 2000  
© Springer-Verlag 2000

**Abstract** In order to study the dynamics of gap junctions in living cells, a cDNA was expressed in hepatocellular carcinoma-derived PLC cells coding for chimerical polypeptide Cx.EGFP-1, which consists of rat connexin32 and enhanced green fluorescent protein (EGFP). Cx.EGFP-1 was integrated into gap junctions, and the emitted epifluorescence reliably reported the distribution of the chimera. Therefore, stably transfected PLC clone PCx-9 was used to examine the dynamic behavior of gap junctions by time-lapse fluorescence microscopy. The pleomorphic fluorescent junctional plaques were highly motile within the plasma membrane. They often fused with each other or segregated into smaller patches, and fluctuation of fluorescence was detected within individual gap junctions. Furthermore, the uptake of junctional fragments into the cytoplasm of live cells was documented as originating from dynamic invaginations that form long tubulovesicular structures that pinch off. Endocytosis and subsequent lysosomal degradation, however, appeared to contribute only a little to the rapid gap junction turnover (determined half-life of 3.3 h for Cx.EGFP-1), since most cytoplasmic Cx.EGFP-1 fluorescence did not colocalize with the endocytosed fluid phase marker horseradish peroxidase or the receptor-specific endocytotic ligand transferrin and since it was distinct from lysosomes. Disassembly of gap junctions was monitored in the presence of the translation-inhibitor cycloheximide and showed increased endocytosis and continuous reduction of junctional plaques. Highly motile cytoplasmic microvesicles, which were detectable as multiple, weakly fluorescent puncta in all movies, are proposed to contribute significantly to gap junction morphogenesis by

the transport of small subunits between biosynthetic, degradative, and recycling compartments.

**Key words** Junction · Connexin · Endocytosis · Green fluorescent protein · Time-lapse microscopy · Live cell recording · Movie · Cell culture

### Introduction

Cell-to-cell communication is a fundamental prerequisite for the coordinated function of all multicellular organisms. Among the many modes of interaction, direct coupling through gap junctions has attracted continued interest. Gap junctions are distinct regions of close cell-to-cell apposition where two unit membranes are separated only by a very narrow gap (Goodenough and Revel 1970). By freeze fracture, clusters of densely spaced membrane particles are seen corresponding to hemichannels, the connexons, which are attached to each other forming gated homo- or heterotypic intercellular pores through which low molecular weight compounds are transported (for recent reviews, see Bruzzone et al. 1996; Goodenough et al. 1996; Kumar and Gilula 1996). Connexons are composed of multiple connexins, a growing group of integral membrane proteins that traverse the membrane four times and that are expressed in a cell-type-restricted fashion in many tissues (Bruzzone et al. 1996; Goodenough et al. 1996). The identification of hereditary diseases that are caused by mutations in connexin genes, the observation of severe defects in connexin knock-out mice and the involvement of gap junctional communication in tumor formation underscore the importance of connexins for tissue development and integrity (for reviews, see Bruzzone et al. 1996; Donaldson et al. 1997; Krutovskikh and Yamasaki 1997; Simon and Goodenough 1998).

Considerable efforts have been directed toward the elucidation of connexin trafficking to understand the modes of regulation of gap-junction-mediated cell communication (Bruzzone et al. 1996; Goodenough et al.

Movies 1–5 can be found at <http://www.uni-mainz.de/FB/Medizin/Anatomie/Leube/>. This work was supported by the Stiftung Rheinland-Pfalz für Innovation

R. Windoffer · B. Beile · A. Leibold · S. Thomas · U. Wilhelm  
R. E. Leube (✉)  
Department of Anatomy, Johannes Gutenberg University Mainz,  
Becherweg 13, D-55099 Mainz, Germany  
e-mail: leube@mail.uni-mainz.de  
Tel.: +49 6131 3922731, Fax: +49 6131 3924615

1996; Laird 1996). Connexins are synthesized in the rough endoplasmic reticulum (ER; Rahman et al. 1993; Falk et al. 1994) where oligomerization can take place, most notably in overexpressing cells (Kumar et al. 1995; for connexin mutants, see also George et al. 1999), although Musil and Goodenough (1993) have shown that connexin43 oligomerizes in the *trans*-Golgi network, probably in small transport vesicles that are on their way to the cell surface. Initial phosphorylation occurs in the ER/Golgi compartments and may be necessary, at least in some cases, for oligomerization and further transport (Puranam et al. 1993; Laird et al. 1995; Koval et al. 1997). Subsequently, connexons are recruited into gap junctions, a finding that seems to correlate with further phosphorylation (Musil and Goodenough 1991; Oyamada et al. 1994; Laird et al. 1995). The intercellular docking of hemichannels relies both on extrinsic factors, such as adhesion molecules, lectins, lipids, calcium and hydrogen atoms, and on intrinsic determinants, such as the cysteine residues in the extracellular loops and the compatibility of the extracellular domains (for reviews, see Bruzzone et al. 1996; Goodenough et al. 1996). Furthermore, distinct stages of gap junction formation have been described corresponding to different forms of arrangement and packing of the compository intramembrane particles (e.g., Benedetti et al. 1974; Johnson et al. 1974, 1989; Fujimoto et al. 1997).

Equally relevant for gap junction modulation are the mechanisms of inactivation involving the removal of junctional plaques from the cell surface, the disassembly of clustered connexons and degradation of connexins, all of which are still poorly understood. In many morphological studies, peculiar vesicular structures have been identified that are surrounded by two unit membranes that are separated by a small gap as in gap junctions (for a review, see Larsen and Risinger 1985). These vesicles have been termed annular gap junctions and it has been proposed that they are formed by the endocytosis of gap junctions, following which the material is degraded, i.e., after fusion with lysosomal vesicles (Larsen and Hai-Nan 1978; Sasaki and Garant 1986; Gregory and Bennett 1988; Naus et al. 1993; see however Severs et al. 1989). An alternative model suggests that the regulation of gap junction removal takes place at the subunit level. Thus, gap junctions may be dispersed within the plasma membrane into junctional fragments or single intramembrane particles that would be available for the reformation of gap junctions or subjected to degradation (Lane and Swales 1980; Fujimoto et al. 1997). Evidence has been presented for different routes of connexin degradation. In the case of connexin43, degradation involves both ubiquitin-mediated proteasomal proteolysis and lysosomal proteolysis (Laing and Beyer 1995; Laing et al. 1997). Furthermore, calpains have been identified as potential degradative enzymes of non-phosphorylated connexin32 (Elvira et al. 1993).

The aim of the current investigation has been the generation of cells to monitor modulations of gap junctions in living cells. The chosen approach is based on the

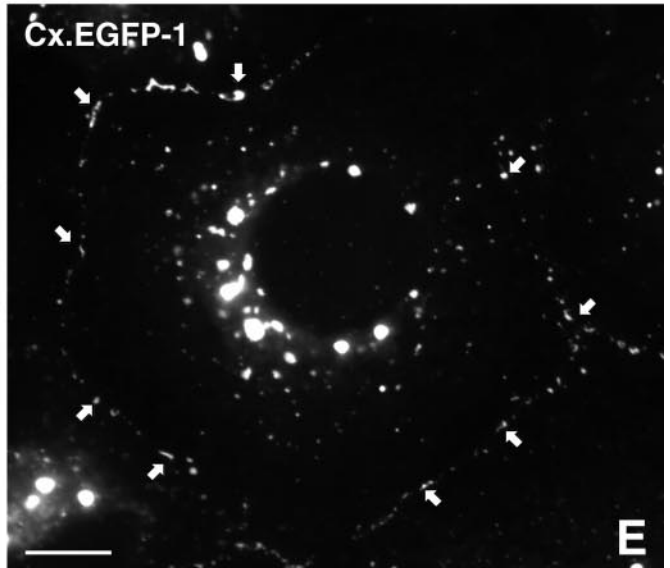
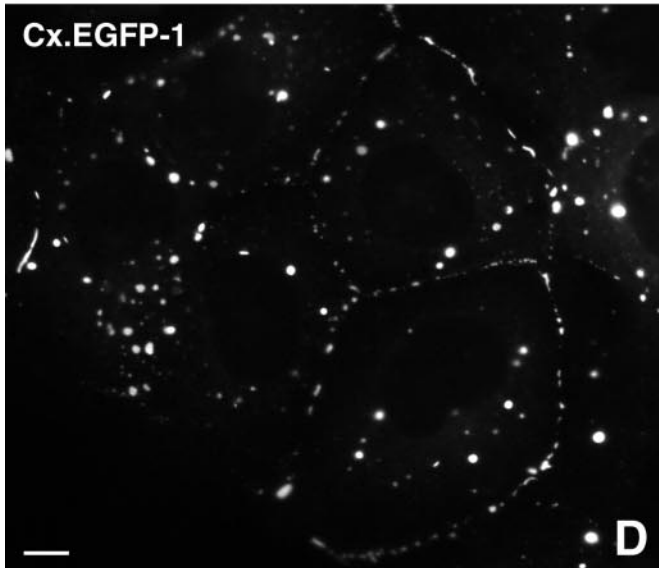
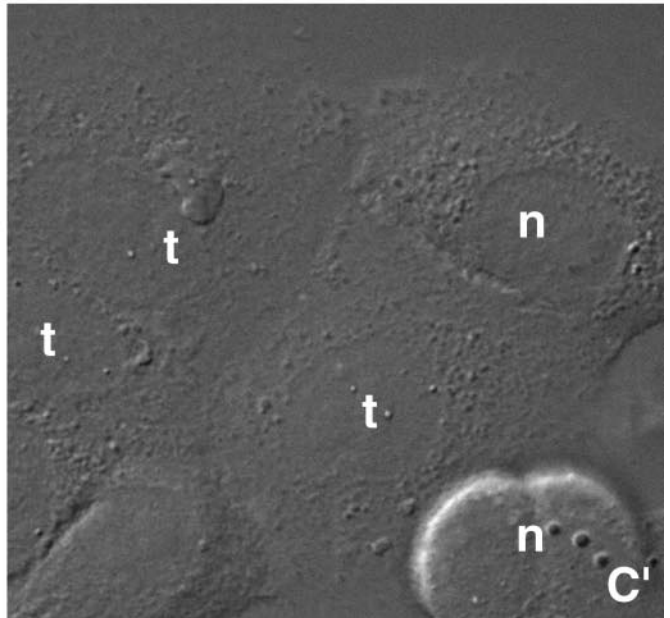
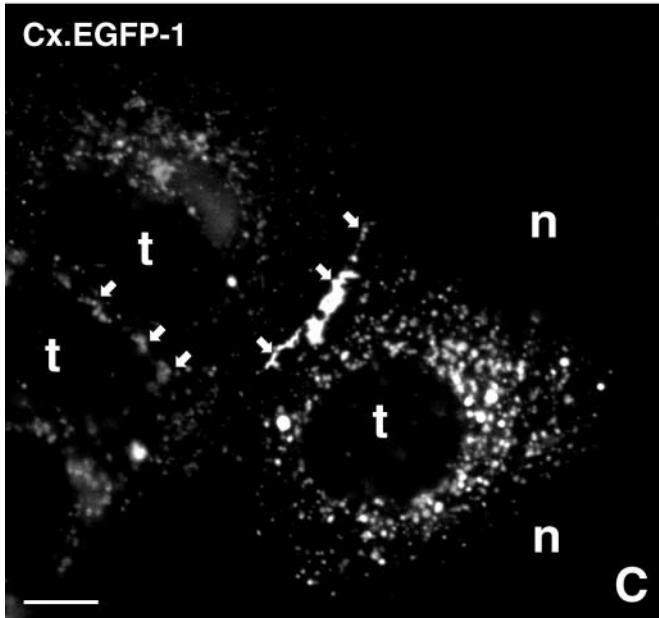
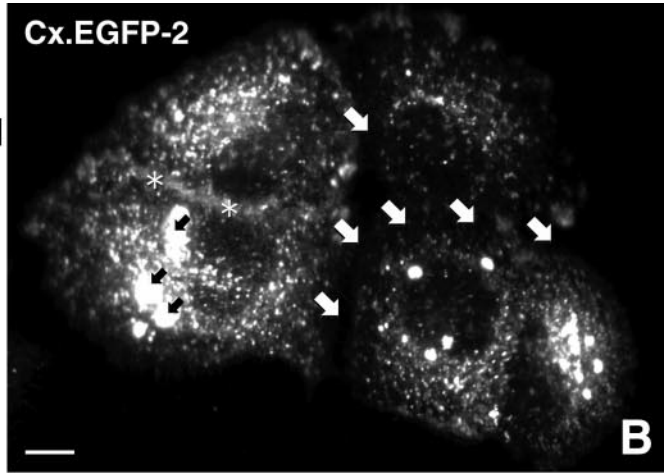
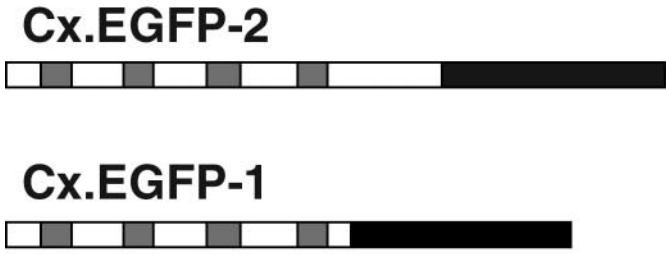
availability of fluorescent polypeptides that can be targeted to specific cellular sites and the finding that connexin molecules and certain connexin mutants induce the formation of functional gap junctions when expressed in heterologous systems by transfection of appropriate DNA constructs or microinjection of cRNA (e.g., Dahl et al. 1987; Swenson et al. 1989; Werner et al. 1989, 1991; Eghbali et al. 1990; Levine et al. 1993; Troyanovsky et al. 1993, 1994a; Rabadan-Diehl et al. 1994; Elfgang et al. 1995; Leube 1995). Therefore, rat liver connexin32 fused to the enhanced green fluorescent protein (EGFP) at its carboxyterminus has been stably introduced into hepatocellular carcinoma cells. The dynamic behavior of this mutant, which is specifically incorporated into characteristic gap junctions, is described by using time-lapse fluorescence microscopy of living cells.

## Materials and methods

### cDNA construction

cDNAs were constructed coding for chimeras consisting of rat connexin32 and EGFP. First, a *HindIII/NarI* fragment of approximately 690 bp was excised from plasmid pCSR1 (Leube 1995) and cloned into the *HindIII/BamHI* sites of pEGFP-N3 (Clontech Laboratories, Palo Alto, Calif.) with the help of oligonucleotides 97–2060 (5'-CGC CG-3') and 97–2061 (5'-GAT CCG G-3'). The resulting plasmid pCx.EGFP-1 encodes chimera Cx.EGFP-1, which is composed of truncated rat connexin32 without its cytoplasmic 63 carboxyterminal amino acids, EGFP, and the short linker sequence GAGFIAL between both elements (Fig. 1A). Expression of the chimeric cDNA is under the control of the immediate early cytomegalovirus promoter. To construct chimera Cx.EGFP-2 (Fig. 1A) encompassing the complete rat connexin32 and EGFP, a fragment of approximately 320 bp was first amplified from pCR1 (Troyanovsky et al. 1993) by polymerase chain reaction (PCR) with oligonucleotides 98–003 (5'-TGC CCC AAC ACA CGG TGG ACT GC-3') and 98–004 (5'-AAA GGA TCC GCA GGC TGA GCA TCG GTC GCT-3'). The *BstXI/BamHI*-digested PCR product was used for replacement of the smaller corresponding fragment of pCx.EGFP-1, thereby generating pCx.EGFP-2. Correct cloning and PCR amplification were confirmed by DNA sequencing in all instances.

**Fig. 1** Schemes of chimeric polypeptides (A) and fluorescence micrographs of living hepatocellular carcinoma-derived PLC cells expressing chimeras Cx.EGFP-2 (B) or Cx.EGFP-1 (C, D, E) either transiently (B, C with corresponding interference contrast picture in C') or stably (D, E). A Transmembrane domains of rat connexin32 are denoted by gray boxes, its cytoplasmic and intravesicular regions by white boxes, and EGFP by a black box. B Note the lack of significant fluorescence of cell borders in most regions (white arrows) and diffuse labeling in some areas (asterisks), the presence of large aggregates in the cytoplasm (black arrows) and the multipunctate cytoplasmic fluorescence in cells expressing Cx.EGFP-2. C, C' Cells transiently expressing Cx.EGFP-1 (*t*) show extensive labeling at adjoining cell borders (arrows) but none at borders to nontransfected interphase and mitotic cells (*n*). In addition, punctate cytoplasmic fluorescence is seen. D, E Note the patches of different sizes at points of cell-to-cell contact (denoted by arrows in E) in cells of clone PCx-9 stably synthesizing Cx.EGFP-1. In addition, vesicular fluorescence of different intensity and size is detectable in the cytoplasm. Bars 10  $\mu$ m



## Cell culture

The hepatocellular carcinoma-derived epithelial cell line PLC (ATCC CRL8024) was grown in DMEM (PAA Laboratories, Cölbe, Germany) supplemented with 10% fetal calf serum (FCS; Life Technologies, Karlsruhe, Germany). DNA transfection was performed with the calcium phosphate precipitation method (cf. Leube 1995), and stably transfected clonal cell lines were picked after selection with geneticin (up to 1 mg/ml; Life Technologies). Sometimes, cells were treated with sodium butyrate (Sigma, St. Louis, Mo.) at 2 mM overnight to increase expression of the transgene. Inclusion of glucose (50 mM) also enhanced gap junction expression. To inhibit protein translation, cells in some experiments were treated with cycloheximide (Sigma; 1 mg/ml stock solution in distilled water) at concentrations between 2.5–40 µg/ml for up to 8 h. In other experiments, Texas-Red-conjugated horseradish peroxidase (HRP; Molecular Probes, Eugene, Ore.) was added as a fluid phase marker to the culture medium at a concentration of 0.1 mg/ml for up to 1 h, and Texas-Red-conjugated transferrin (Molecular Probes) was used as a receptor-specific ligand at concentrations of 1.25, 2.5, and 5 µg/ml for up to 1 h.

## Antibodies and immunofluorescence microscopy

Rabbit polyclonal antibodies against green fluorescent protein (GFP) were from Molecular Probes, rabbit antibodies against a synthetic peptide corresponding to the first cytoplasmic loop of rat connexin32 from Dr. V. Krutovskikh (Krutovskikh et al. 1994), and murine monoclonal antibodies against the lysosomal membrane protein LAMP-2 (hybridoma H4B4) from the Developmental Studies Hybridoma Bank (Iowa City, Iowa). Secondary antibodies, viz., Texas-Red-conjugated goat anti-mouse IgG and Texas-Red-conjugated goat anti-rabbit IgG, were purchased from Jackson ImmunoResearch Laboratories (West Grove, Pa.). For indirect immunofluorescence microscopy, cultured cells were grown on glass coverslips, fixed with formaldehyde, lysed with digitonin, and incubated with antibodies as described recently (Windoffer et al. 1999). Fluorescence was viewed in an epifluorescence microscope (Axiophot, Carl Zeiss, Jena, Germany) and recorded with a digital camera (Orca 4742–95, Hamamatsu, Herrsching, Germany).

## Immunoelectron microscopy

For immunoelectron microscopy, cells grown to high density on glass coverslips were briefly washed in phosphate-buffered saline (PBS; 37°C) and fixed at room temperature for 10 min in 2% formaldehyde freshly prepared in PBS. After 2×5 min washes in PBS, cells were treated with 0.1% saponin (Sigma) in PBS at room temperature for 5 min and washed again twice with PBS. Unspecific antibody binding sites were blocked by incubation in 5% normal goat serum (Sigma) in PBS for 15 min. After a wash with PBS, rabbit anti-GFP antibodies (1:8 000 in PBS) were applied for 2 h (omitted in negative control). The cells were washed (3×5 min) in PBS before being incubated with secondary 1 nm gold-conjugated goat anti rabbit-IgG antibodies (1:50 in PBS; Nanoprobes, Stony Brook, NY) overnight at 4°C. After three washes in PBS (each 5 min), a second fixation step was carried out (2.5% glutaraldehyde in PBS for 15 min at room temperature). For silver enhancement, cells were washed (2×10 min) in HEPES buffer (50 mM HEPES, 200 mM sucrose, pH 5.8), treated with HQ Silver (Nanoprobes) for 6 min, and washed (2×5 min) in a solution containing 50 mM HEPES and 250 mM sodiumthiosulfate (pH 7.5) followed by 2×5 min washes in PBS. For final fixation, 0.2% osmium tetroxide was applied for 30 min at room temperature and was then washed out with distilled water. Cells were dehydrated in a graded ethanol series, passed through propylene oxide, and embedded in Epon 812. Ultrathin sections were prepared with a Reichert-Jung Ultramicrotome (Leica, Bensheim, Germany) and lightly stained with 8% uranyl acetate (in water) for

10 min. Grids were viewed and documented in an EM10 electron microscope (Carl Zeiss).

## Time-lapse fluorescence microscopy

To view living cells, a self-made culture chamber was screwed tightly onto the stage of an epifluorescence microscope (Axiophot, Carl Zeiss). The chamber ( $V=500\ \mu\text{l}$ ) consisted of a steel frame with holes for the exchange of culture medium and for a sensor to record continuously the temperature close to the cell monolayer. The bottom of the chamber was located on top of another glass chamber that could be perfused with preheated water to maintain the culture chamber precisely at 37°C. A coverslip was placed on top of the culture chamber so that the adhering cells grew in an inverted position. During recording, cells were maintained in phenol-red-free Hanks' medium containing Hanks' salt solution, 25 mM HEPES, MEM non-essential amino acid solution, MEM amino acid solution, 100 U/ml penicillin, 100 µg/ml streptomycin (all from Life Technologies), 5% FCS, and 4.8 mM N-acetyl-L-cysteine (Sigma), pH 7.4. To improve the stability of the fluorescence, ascorbic acid (0.5 mg/ml, Sigma) was added to the medium. The culture medium was exchanged either continuously or in single steps by using a pump with adjustable flow rates.

EGFP epifluorescence was recorded by using filterset no. 10 from Zeiss and a digital camera (see above). HPD-CPx software (Hamamatsu) was used to obtain the images and to control a shutter (Zeiss). In some instances, a brightfield picture was recorded immediately before each fluorescence image. The resulting image sequences were edited with Image-Pro Plus 4.0 software (Media Cybernetics, Silver Spring, Calif.) and converted into movies (QuickTime 3.0). They are available at <http://www.uni-mainz.de/FB/Medizin/Anatomie/Leube/>. Photoshop software (Adobe Photoshop 5.0) was used to edit single pictures and to compose tables.

## Cell fractionation, immunoblotting, and pulse-chase labeling

For cell fractionation, confluent cell monolayers were washed twice with ice cold PBS. Ice-cold hypotonic buffer, consisting of 10 mM TRIS-HCl pH 7.4, 1 mM EGTA, 1 mM EDTA, 2 mM dithiothreitol (DTT), 0.1 mg/ml phenylmethane sulfonyl fluoride (PMSF), and 0.2 mg/ml 4-(2-aminoethyl)-benzenesulfonyl fluoride, was added directly to the culture dish after removal of PBS. Lysed cells were scraped off and homogenized by 30 up and down strokes in a tight-fitting Dounce homogenizer. Nuclei were pelleted by centrifugation at 1000 g at 4°C for 15 min. The resulting supernatant was then centrifuged at 10,000 g for 1 h at 4°C. The 10,000 g pellet was resuspended in hypotonic buffer, and the supernatant was subjected to another round of centrifugation (100,000 g for 1 h at 4°C). The 100,000 g pellet was also dissolved in hypotonic buffer. Protein concentrations were determined by using the BioRad reagent (BioRad Laboratories, Munich, Germany). The polypeptides were solubilized in loading buffer (2% SDS, 150 mM DTT, 0.005% bromophenol blue, 30 mM TRIS-HCl pH 6.8, 10% glycerol) and 50 µg was loaded per lane onto a 12% SDS polyacrylamide gel. After electrophoresis, polypeptides were transferred to nitrocellulose by electroblotting. The membranes were first preadsorbed with 5% low fat milk powder in PBS. They were then incubated with primary antibodies in PBS together with 5% low fat milk powder, washed several times, and subsequently incubated with HRP-coupled secondary antibodies (Jackson-ImmunoResearch Laboratories). Bound antibodies were detected with an enhanced chemiluminescence system (Pharmacia Amersham Biotech, Freiburg, Germany).

For pulse-chase experiments, cells were grown to near confluence in Petri dishes (9 cm diameter). They were first treated with methionine-free DMEM (Life Technologies) supplemented with 10% FCS for 45 min. Subsequently, cells were pulse-labeled by incubation in methionine-free medium (5 ml/Petri dish) with 10% FCS and 100 µCi/ml <sup>35</sup>S-methionine (>1000 Ci/mmol; Amersham

Pharmacia Biotech) for 2 h. Afterwards, cells were washed three times in methionine-reduced medium, i.e., methionine-free DMEM with 10% FCS and 1 mM methionine (prepared from 20 mM L-methionine solution; Sigma). Cells were then either harvested directly or after various chase periods (incubation in methionine-reduced medium). At the end of the respective chase periods, cells were washed several times with ice-cold PBS. Cells were first lysed in 1.5 ml/dish RIPA buffer (10 mM monosodium phosphate pH 7.2, 150 mM NaCl, 2 mM EDTA, 1% (v/v) Triton X-100, 0.25% (w/v) SDS, 1% (w/v) sodium deoxycholate, 2 mM PMSF) by repeated resuspension and incubation on ice for at least 20 min. The subsequent steps were all performed at 4°C with pre-cooled solutions. Non-solubilized material was pelleted by centrifugation (100,000 g, 30 min). Equal polypeptide amounts of the resulting supernatant were subjected to a pre-clearing step by incubation with 15–20 mg protein-A-sepharose (type CL-4B; Amersham Pharmacia Biotech) that had been pre-swollen in RIPA buffer. The sepharose was briefly spun down (3500 rpm in a table-top centrifuge, 3 min), and the resulting supernatants were incubated with anti-GFP antibody for 2–3 h with constant agitation (primary antibodies were omitted in control samples). Subsequently, 15–20 mg protein-A-sepharose suspended in RIPA buffer was added, and incubation was continued for another hour. The sepharose was then washed 2–5 times with wash buffer 1, consisting of 0.5% (w/v) Tween-20, 50 mM TRIS-HCl pH 7.5, 150 mM NaCl, 0.1 mM EDTA, 2–3 times with wash buffer 2, consisting of 0.5% (w/v) Tween-20, 100 mM TRIS-HCl pH 7.5, 200 mM NaCl, 2 M urea, and once with distilled water. Between each step, sepharose was pelleted by a brief low-speed centrifugation. The pelleted and washed material was then dissolved directly in loading buffer (see above) and boiled for 5 min; equal amounts were loaded onto 10% SDS polyacrylamide gels. After electrophoresis, polypeptides were stained with Coomassie Blue, and the gels were dried and subjected to autoradiography. Gel regions containing the immunoprecipitates and the corresponding areas in control lanes were precisely excised and dissolved in scintillation liquid; radioactivity was measured for 15 min in a  $\beta$ -counter to determine the time-course of degradation.

## Results

### Formation of fluorescent gap junctions in living cells

When chimera Cx.EGFP-2 (Fig. 1A) consisting of the entire coding region of rat connexin32 and EGFP was expressed in hepatocellular carcinoma-derived PLC cells, a multipunctate cytoplasmic fluorescence was seen with some large aggregates, whereas cell borders were either not stained at all or only diffusely fluorescent (Fig. 1B), indicating that the chimeric polypeptides were not integrated into gap junctions. Therefore, a second construct was prepared with a truncated version of connexin32, since recent studies have shown that deletion and/or substitution of the cytoplasmic carboxyterminus does not interfere with either the topogenesis or function of connexin32 (Werner et al. 1991; Levine et al. 1993; Troyanovsky et al. 1993, 1994a, 1994b; Rabadan-Diehl et al. 1994; Leube 1995; George et al. 1998, 1999). The segment used for the expression of Cx.EGFP-1 (Fig. 1A) was identical to that used by us recently (Troyanovsky et al. 1993, 1994a, 1994b; Leube 1995) but was one amino acid longer than the shortest, still fully functional, mutant described by Rabadan-Diehl et al. (1994), 10 amino acids longer than the chimera investigated by George et al. (1998, 1999), and 5 amino acids shorter than the mu-

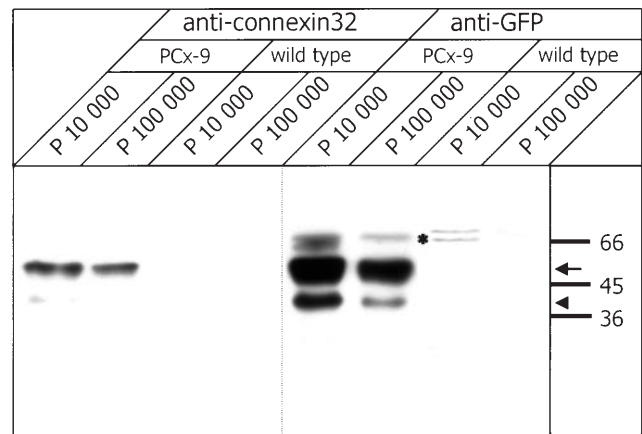


**Fig. 2** Photographs of immunoblots obtained from cell fractions that were prepared from hepatocellular carcinoma-derived PLC wild type cells (*wild type*) and subclone *PCx-9* stably transfected to express chimera Cx.EGFP-1. The chimera was detected either with antibodies against connexin32 (*anti-connexin 32*) or GFP (*anti-GFP*). The 10,000 g pellet fractions (*P 10 000*) and 100,000 g pellet fractions (*P 100 000*) were subsequently prepared, and equal polypeptide amounts were loaded in each lane. Note that both antibodies react with a polypeptide of the expected size of approximately 53 kDa (*arrow*) and more weakly with a lower molecular weight polypeptide (*arrowhead*). The additional slower migrating bands seen with the GFP antibody are unspecific as they are also detectable in wild type cells (*star*). The position and molecular mass of co-electrophoresed size markers are shown *right* in kDa

tant examined by Werner et al. (1991) and Levine et al. (1993). Similar to our previous observations, chimeric polypeptides were detectable in strongly fluorescent membrane patches of various sizes at cell borders and in multiple vesicular elements of variable appearance (Fig. 1C, C'). No plasma membrane staining was observed between transfected and non-transfected cells (Fig. 1C, C'). Next, stably transfected cell lines were selected to minimize the cell-to-cell variation in transgene expression and polypeptide distribution. The fluorescence seen in living cells of one such clone is depicted in Fig. 1D, E. The results obtained with this clone, termed *PCx-9*, are presented in the rest of this communication, although similar results were obtained in other cell lines that were established in parallel.

When polypeptides enriched in 10,000 g and 100,000 g pellets from *PCx-9* cells were analyzed by immunoblotting, a major polypeptide band reacted with antibodies directed against GFP and connexin32; this band migrated in the expected molecular weight range (calculated molecular weight of fusion protein 52,718; Fig. 2). In addition, some lower molecular weight bands were detected with both antibodies; these bands possibly resulted from aberrant processing in the ER as reported for cells overexpressing connexin32 (Falk et al. 1994) or from degradation and/or modification. Most immunoreactivity was found in the 10,000 g pellet fraction. No connexin polypeptides were detected in wild type PLC cells.

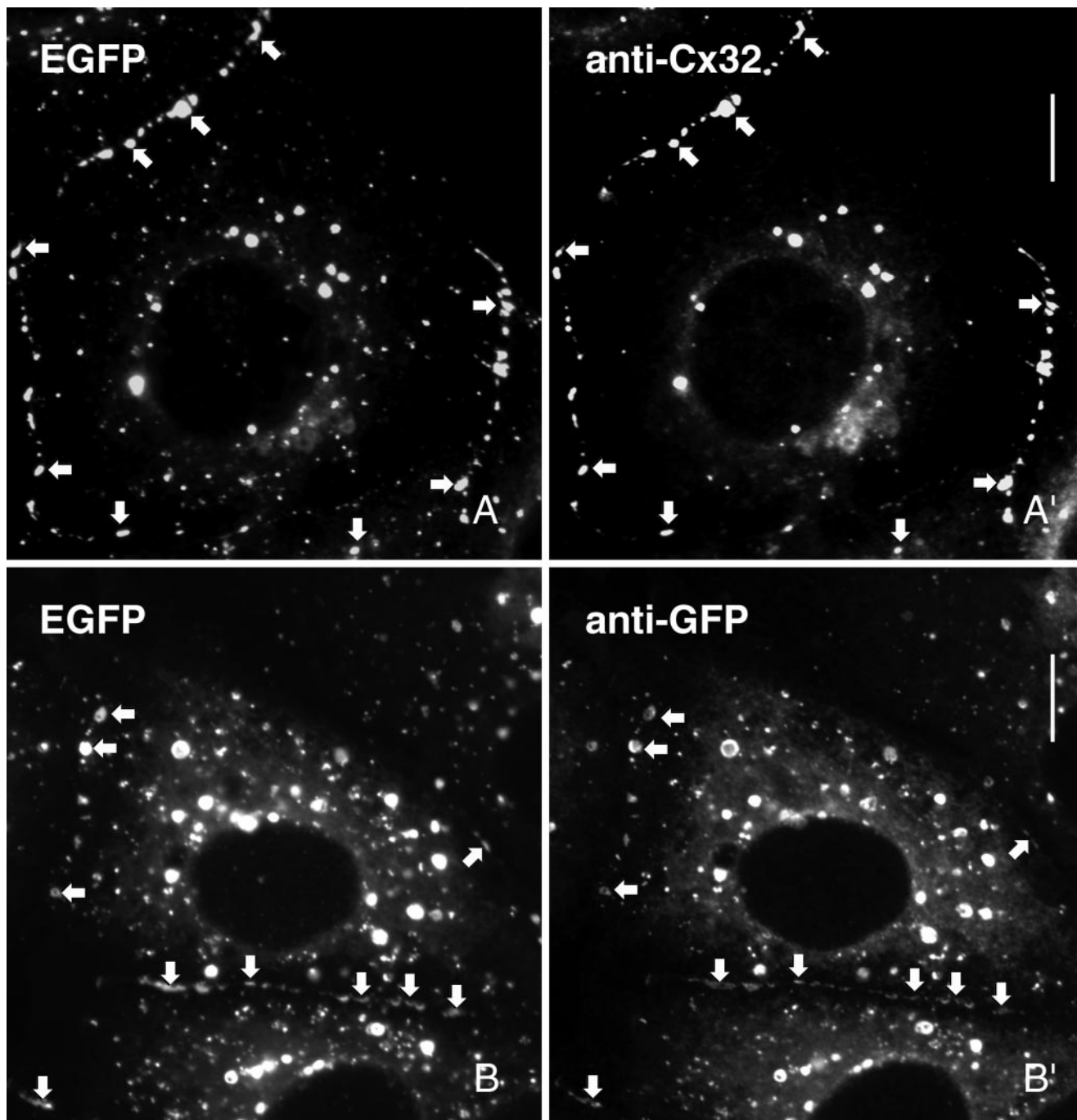
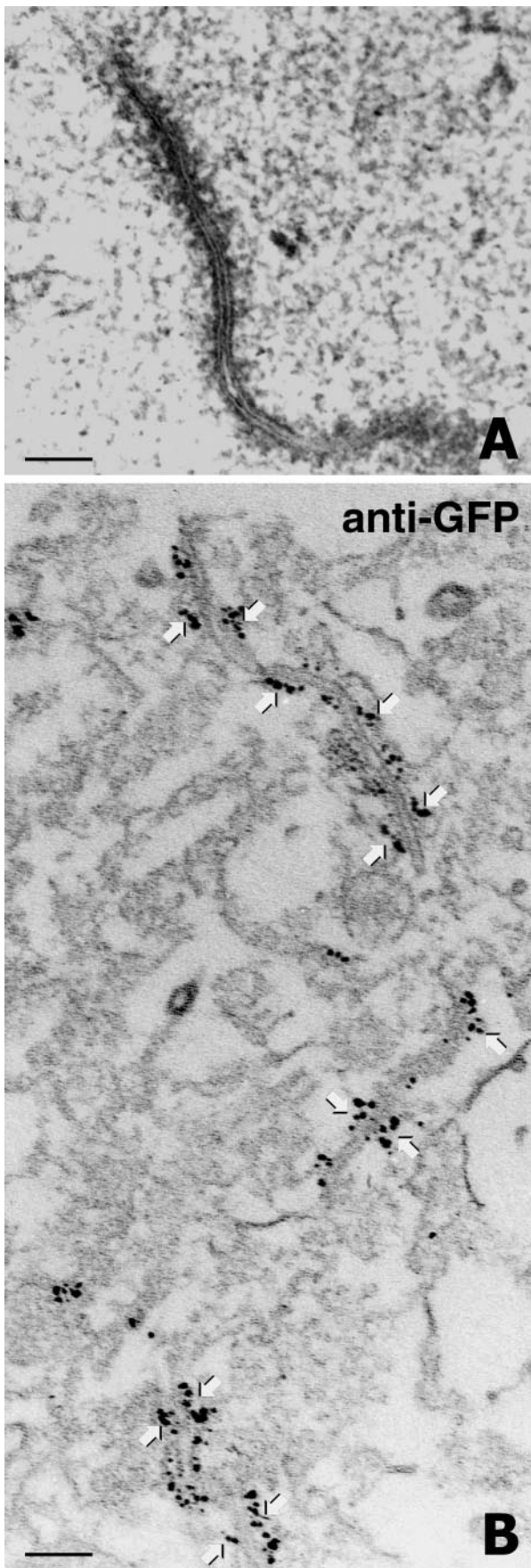


**Fig. 3** Fluorescence micrographs showing EGFP fluorescence (**A**, **B** *EGFP*) and corresponding indirect immunofluorescence with antibodies against connexin32 (**A'** *anti-Cx32*) or GFP (**B'** *anti-GFP*) in formaldehyde-fixed PLC cells of clone PCx-9 stably expressing Cx.EGFP-1. Note that the EGFP-fluorescence coincides in most part with the epitopes detected by indirect immunofluorescence, although the connexin antibodies do not detect all EGFP-positive structures. (Arrows Fluorescent plaques at cell contact sites.) Bars 10  $\mu$ m

The fluorescence pattern of Cx.EGFP-1 was retained after fixation and was indistinguishable from that seen in live cells (compare, e.g., Fig. 1D, E with Fig. 3A, B). Furthermore, the strong fluorescence emitted by the chimeric polypeptides almost completely co-localized with the immunofluorescence obtained by using antibodies against connexin32 or GFP (Fig. 3), although the sensitivity of the connexin antibodies was not sufficient to detect all fluorescent Cx.EGFP-1. It was concluded that GFP-fluorescence can be used as a highly sensitive and reliable marker for tracking Cx.EGFP-1 in PCx-9 cells.

We then showed, by electron microscopy, that, in contrast to wild type PLC cells, multiple large gap junctions



are present in PCx-9 cells. In some instances, the characteristic multilaminar structure was resolved (Fig. 4A). Furthermore, these gap junctions contained the chimeric polypeptide as seen by immunoelectron microscopy (Fig. 4B). Labeling was also detectable in cytoplasmic vesicles, including vesicular profiles, which were partially surrounded by two or multiple layers of closely apposed unit membranes (not shown).

#### Dynamics of gap junctional plaques

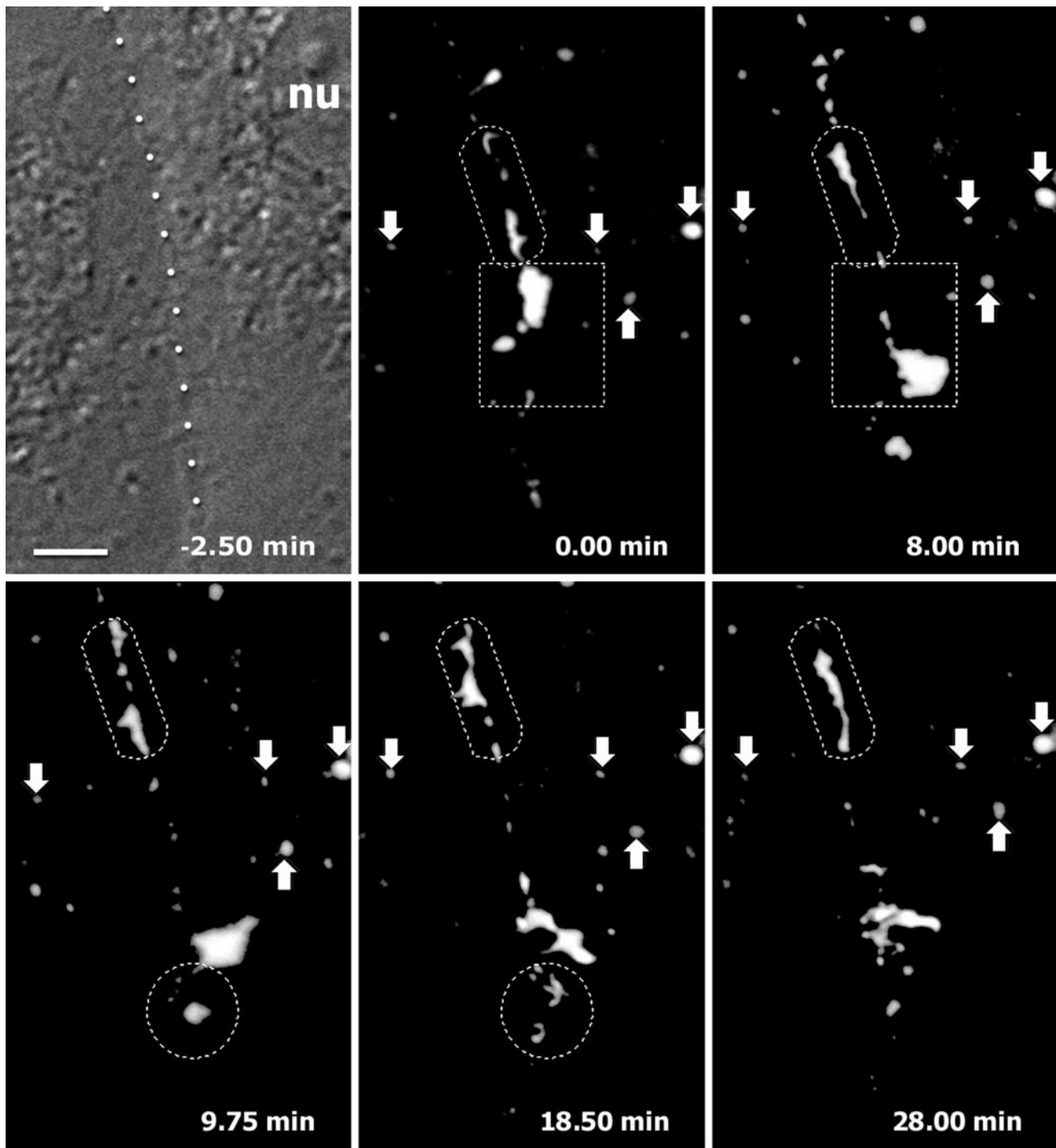
To record the dynamics of Cx.EGFP-1-containing structures by time-lapse fluorescence microscopy, PCx-9 cells were placed in a small chamber that was mounted on the stage of an epifluorescence microscope; fluorescence was monitored with a digital camera. Figure 5 presents a selection of pictures taken from a typical series of micrographs that were recorded at 15-s intervals for 28 min. The movie generated from these pictures (movie 1; available at <http://www.uni-mainz.de/FB/Medizin/Anatomie/Leube/>) shows that the multiple fluorescent plaques at the cell border between the two cells are highly dynamic. Most move around erratically and change their shape continuously (see, e.g., region marked by rectangle in Fig. 5 and movie 1). They often fuse with each other (see, e.g., regions marked by ovoids in Fig. 5 and movie 1) or separate into small parts (see, e.g., region marked by circle in Fig. 5 and movie 1). In contrast to the high degree of mobility of gap junctions at the cell surface, several large and strongly fluorescent cytoplasmic structures were stationary, moving only very little during the entire observation period (e.g., arrowheads in Fig. 5). In addition, many small puncta were detectable, most of which were labeled very weakly and are just above the detection limit. These multiple vesicular elements moved around in the cytoplasm rapidly (movies 1–4 at <http://www.uni-mainz.de/FB/Medizin/Anatomie/Leube/>) and were difficult to follow between frames.

Movie 2 taken at 0.14-min intervals and the corresponding Fig. 6 depict another type of behavior of dynamic gap junctions. In this short sequence, two fluorescent plaques can be viewed *en face*, thereby showing differences in fluorescence intensity within the extended contact regions. Circular spots of increased or reduced intensity can be distinguished from weaker fluorescence, all of which move and intermingle quickly.

#### Endocytosis of gap junctional plaque regions

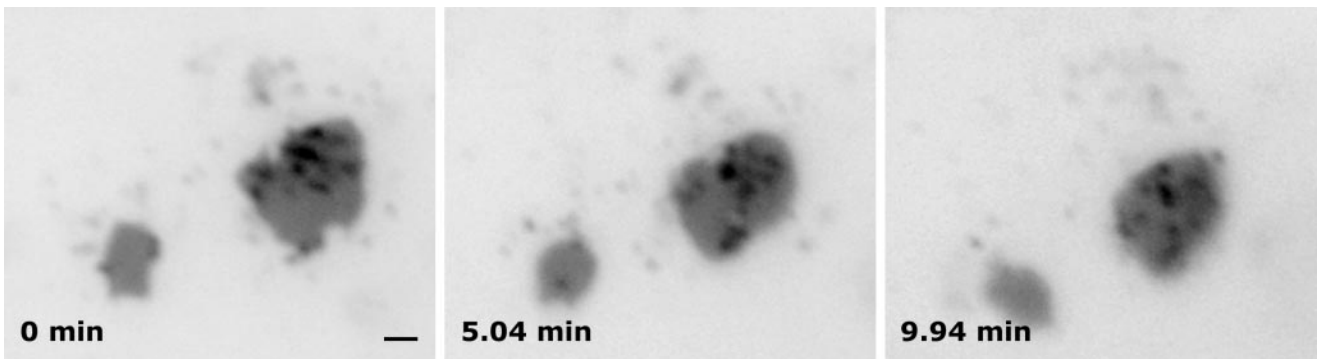
In order to understand the relationship between the surface-localized gap junctions and the multiple fluorescent

**Fig. 4** Electron microscopy (A) and immunoelectron microscopy (B) of PLC clone PCx-9 stably expressing chimera Cx.EGFP-1. A Gap junction with characteristic multilaminar appearance. B Multiple gap junction-like structures (arrows) labeled by antibodies against GFP (*anti-GFP*) with the immunogold technique in combination with silver amplification. Bars 150 nm



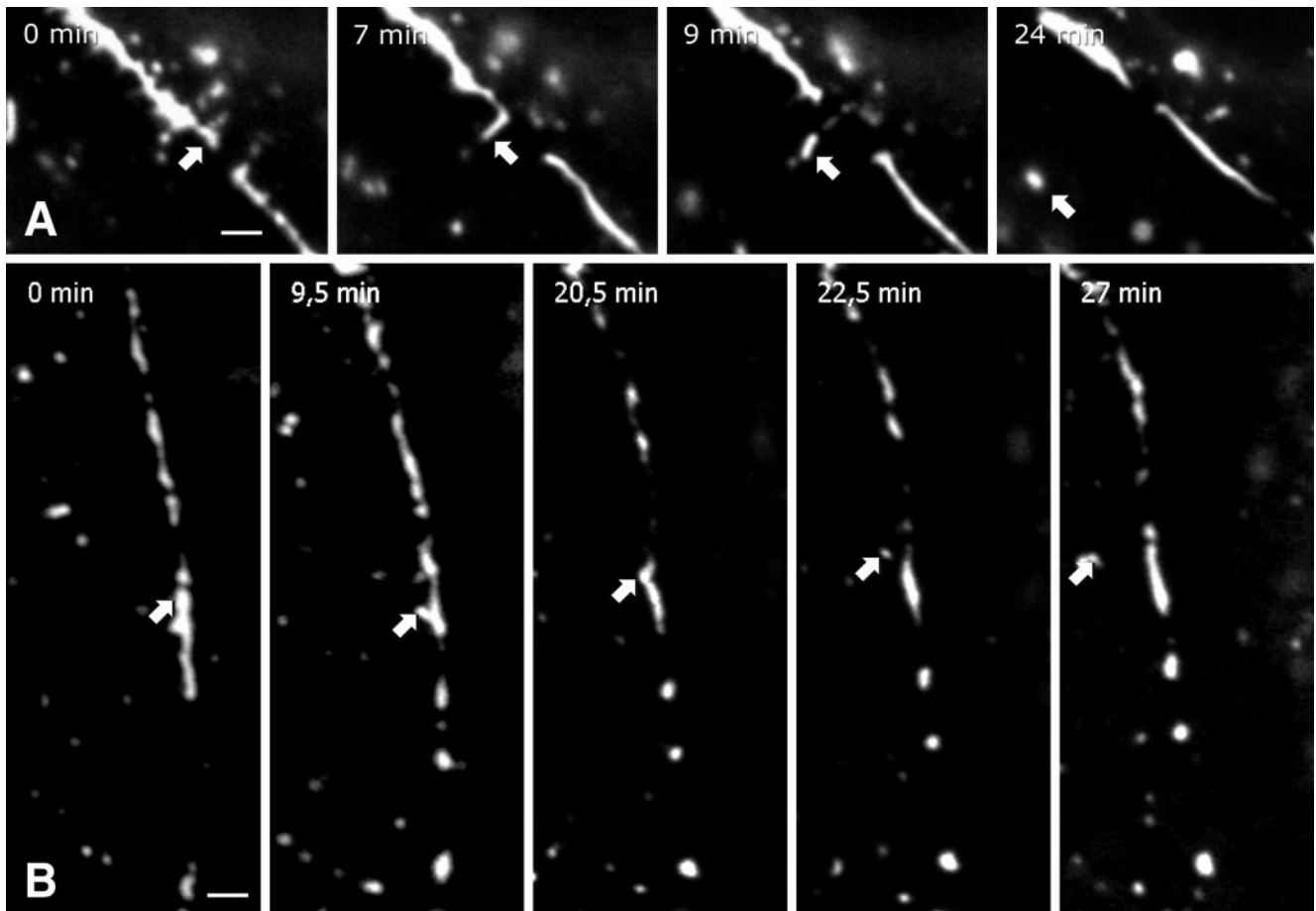
**Fig. 5** Sequence of fluorescence micrographs taken from movie 1 (pictures taken every 0.25 min for 28 min; available at <http://www.uni-mainz.de/FB/Medizin/Anatomie/Leube/>) documenting the dynamics of Cx.EGFP-1-positive structures in living PLC cells of clone PCx-9. The brightfield picture was taken 2.50 min before the start of fluorescence microscopy, and the position of the cell border between both cells is demarcated by the *dotted line* (*nu* position of nucleus). Note the different types of mobility of fluorescent patches at cell contact sites that are best resolved in the movie. In both the figure and movie, a region of high mobil-

ity is labeled by a *rectangle*, the fusion of plaques is demarcated by an *ovoid* between 0.00 min and 9.50 min and again in another area by an *ovoid* between 9.75 min and 28.00 min. Separation of a plaque into several fragments is marked by a *circle*. The time points of recording are given *lower right* in minutes. Some large, strongly fluorescent cytoplasmic structures that remain stationary are denoted by *arrows* only in the figure. Note also the presence of many rapidly moving small fluorescent dots in the movie. *Bar* 5  $\mu$ m



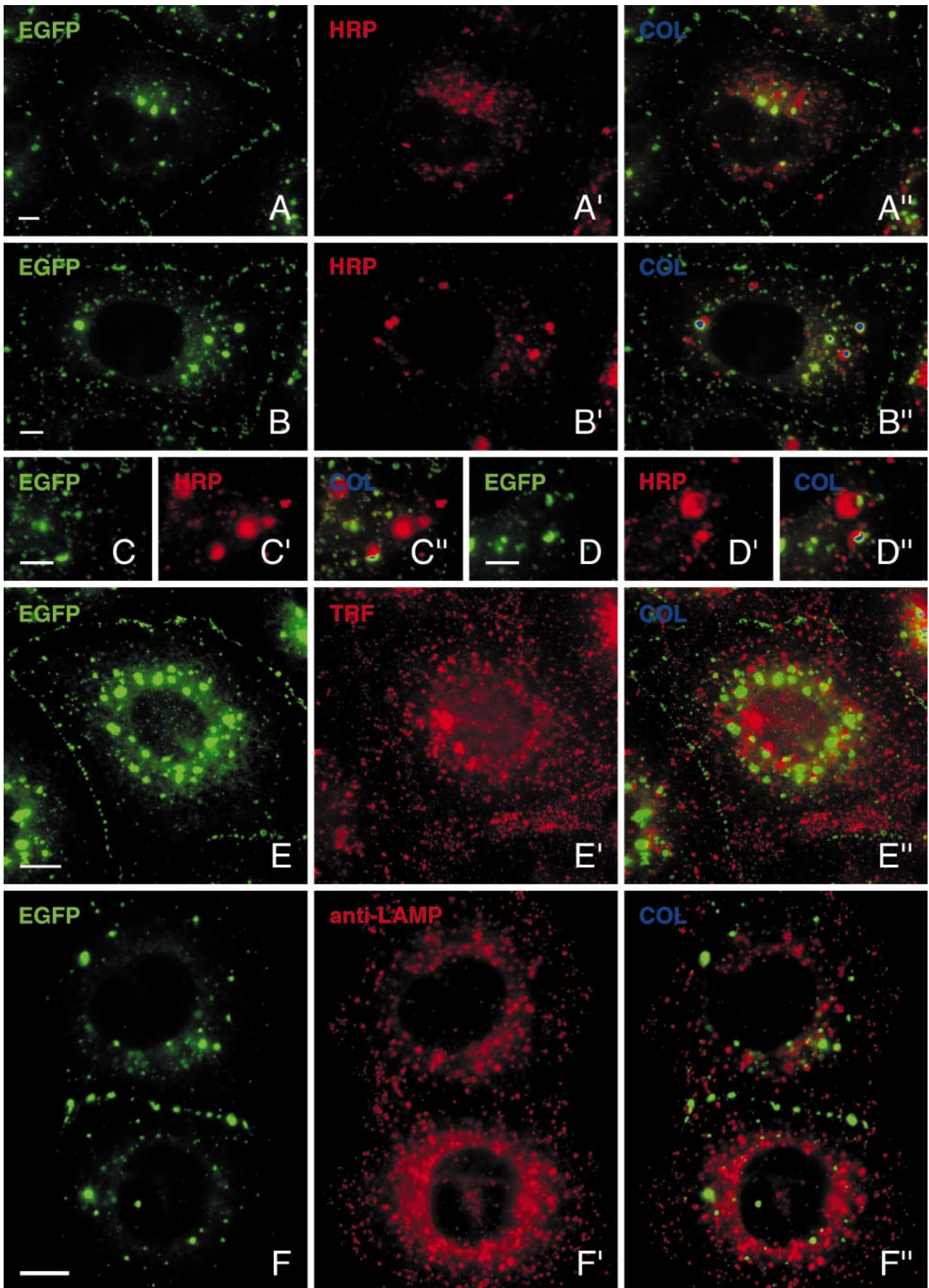
**Fig. 6** Fluorescence micrographs (inverse presentation) depicting heterogeneity in two Cx.EGFP-1-positive cell contact sites that are viewed *en face* in live PLC cells of clone PCx-9. The three pictures shown are taken from a short 9.94 min movie (movie 2; accessible at <http://www.uni-mainz.de/FB/Medizin/Anatomie/Leube/>) for which

pictures were recorded every 0.14 min. The time of recording is given *lower left*. Note the differences in fluorescence intensity, particularly in the large structures *right* that are seen to move around in the movie. Weak and highly mobile fluorescence is also detectable in the vicinity corresponding to cytoplasmic regions. *Bar* 1  $\mu\text{m}$



**Fig. 7A, B** Pictures taken from time-lapse fluorescence microscopy of Cx.EGFP-1-expressing PCx-9 cells depicting endocytosis of gap junctional fragments. The sequence in **A** (corresponding movie 3 taken at 1 min intervals; available at <http://www.uni-mainz.de/FB/Medizin/Anatomie/Leube/>) shows the budding of a tubular structure from an extensive junction (*arrow* in figure and movie). In **B** (corresponding movie 4 taken at 0.5 min intervals; available at <http://www.uni-mainz.de/FB/Medizin/Anatomie/Leube/>), a strongly fluorescent patch (*arrow* in figure and movie) can be tracked within a gap junction that first extends into the cytoplasm (9.5 min), retracts (20.5 min) before it eventually buds off (22.5 min), and is taken up into the cytoplasm (27 min). *Bar* 2  $\mu\text{m}$

cytoplasmic vesicular structures in PCx-9 cells, we focused our attention on possible exo- and endocytotic fusion events. Given the limits of spatial and temporal resolution obtainable in the current experimental setup, it was difficult to trace the very small vesicles, which not only moved extremely rapidly, but also passed in and out of the focal plane. Therefore, it was only possible unambiguously to follow the movements of the larger and strongly fluorescent vesicles. In contrast to the absence of documentable exocytotic fusion of any of these vesi-



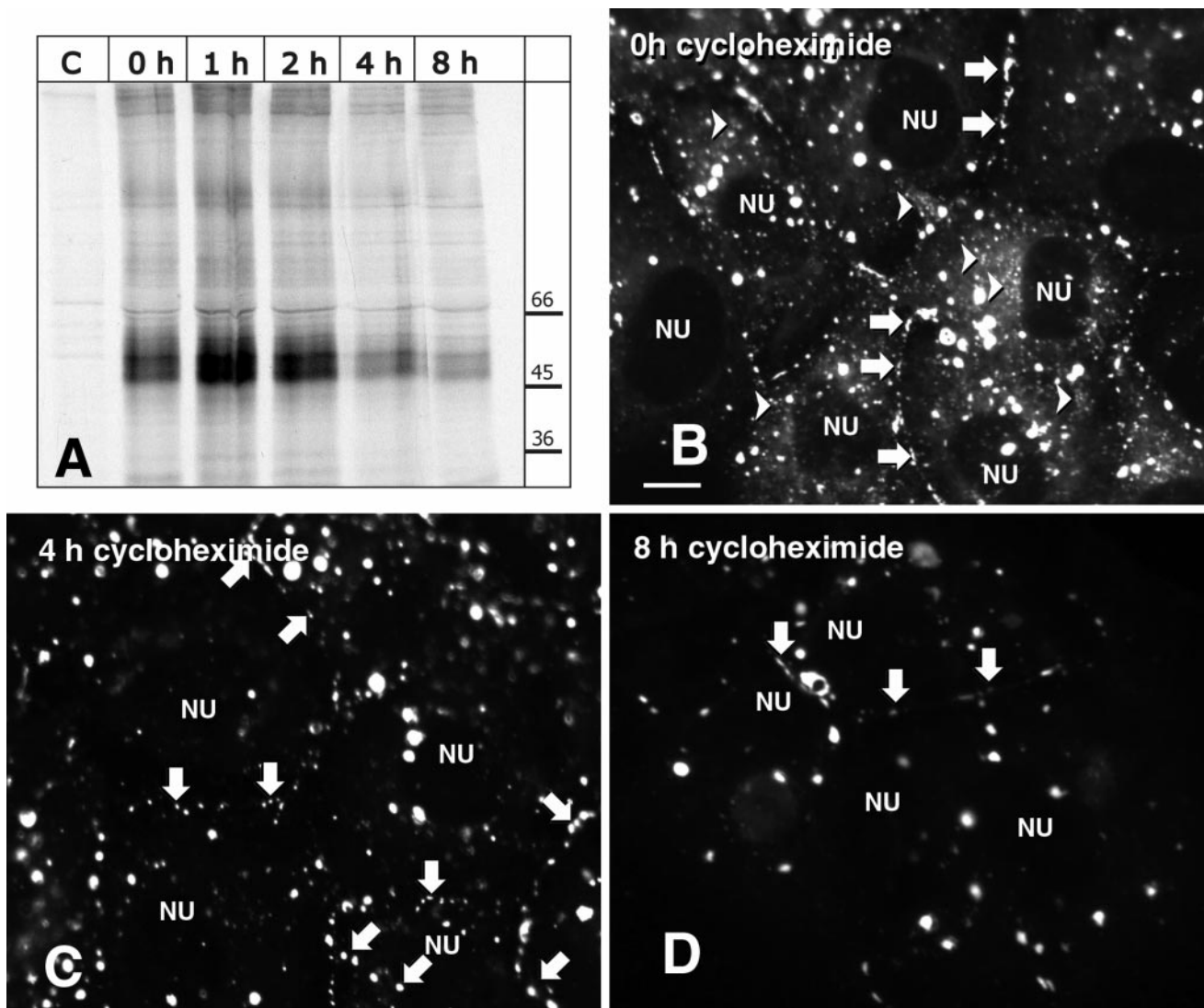


**Fig. 9** Composite autoradiograph of immunoprecipitates obtained from pulse-labeled PCx-9 cells to determine the half life of Cx.EGFP-1 (A) and fluorescence microscopy of formalin-fixed PCx-9 cells treated with cycloheximide (B–D). A Immunoprecipitates using GFP-specific antibodies were prepared from pulse-labeled cells after various chase periods (0h, 1h, 2h, 4h, 8h) and separated by 10% SDS PAGE (right position and molecular mass in kDa of co-electrophoresed molecular weight standards). Note the decrease in intensity of bands after 1 h and the lack of significant radioactivity in the control lane (C) prepared from immunoprecipitates without primary antibodies. Higher molecular weight bands

correspond to connexin multimers that were not completely resolved in this experiment. B–D Fluorescence micrographs showing continuous loss of Cx.EGFP-1 fluorescence in PCx-9 cells in the presence of cycloheximide (17.5 µM). Note that perinuclear and fine vesicular immunoreactivities, which are seen at the onset of the experiment (0h; arrowheads in B), are no longer detectable at 4 h and that an overall progressive reduction of immunoreactivity is apparent at 4h and 8h, both at cell contact sites (compare arrows in B–D) and in the large cytoplasmic vesicular structures (NU position of nucleus). Bar 10 µm (all micrographs)

◀ **Fig. 8** Fluorescence microscopy depicting the distribution of Cx.EGFP-1 (A–F) in formalin-fixed PLC cells of clone PCx-9 in relation to endocytosed Texas-Red-labeled HRP (0.1 mg/ml for 1 h; A', B', C', D'), endocytosed Texas-Red-labeled transferrin (5 µg/ml for 1 h; E') and the lysosomal marker LAMP-2 detected by indirect immunofluorescence microscopy (F'). The third picture in each case was generated by overlay, and co-localization of green and red fluorescent spots is shown in a false blue color for the better identification of the very rare colocalizing fluorescent spots. Note that significant colocalization was only seen in some cases for endocytosed HRP and Cx.EGFP-1 (e.g., B'') and that, in these instances, EGFP fluorescence often formed a partial cap on HRP-labeled vesicles (see high magnification in C'' and D''). Bars 5 µm in A, B; 2 µm in C, D; 10 µm in E, F

cles, the occasional endocytosis of partial gap junctions was seen. Two examples are depicted in Fig. 7 and movies corresponding 3 and 4 revealing some remarkable features. Figure 7A shows that a local concentration of fluorescence within a plaque region is visible long before endocytosis occurs. This junctional microdomain moves around within the junction and forms extensive tubular infoldings, flattening out several times before it eventually buds off. An elongated budding profile is also seen in Fig. 7B. The endocytotic structures are then taken deep into the cytoplasm, change shape, and round up.

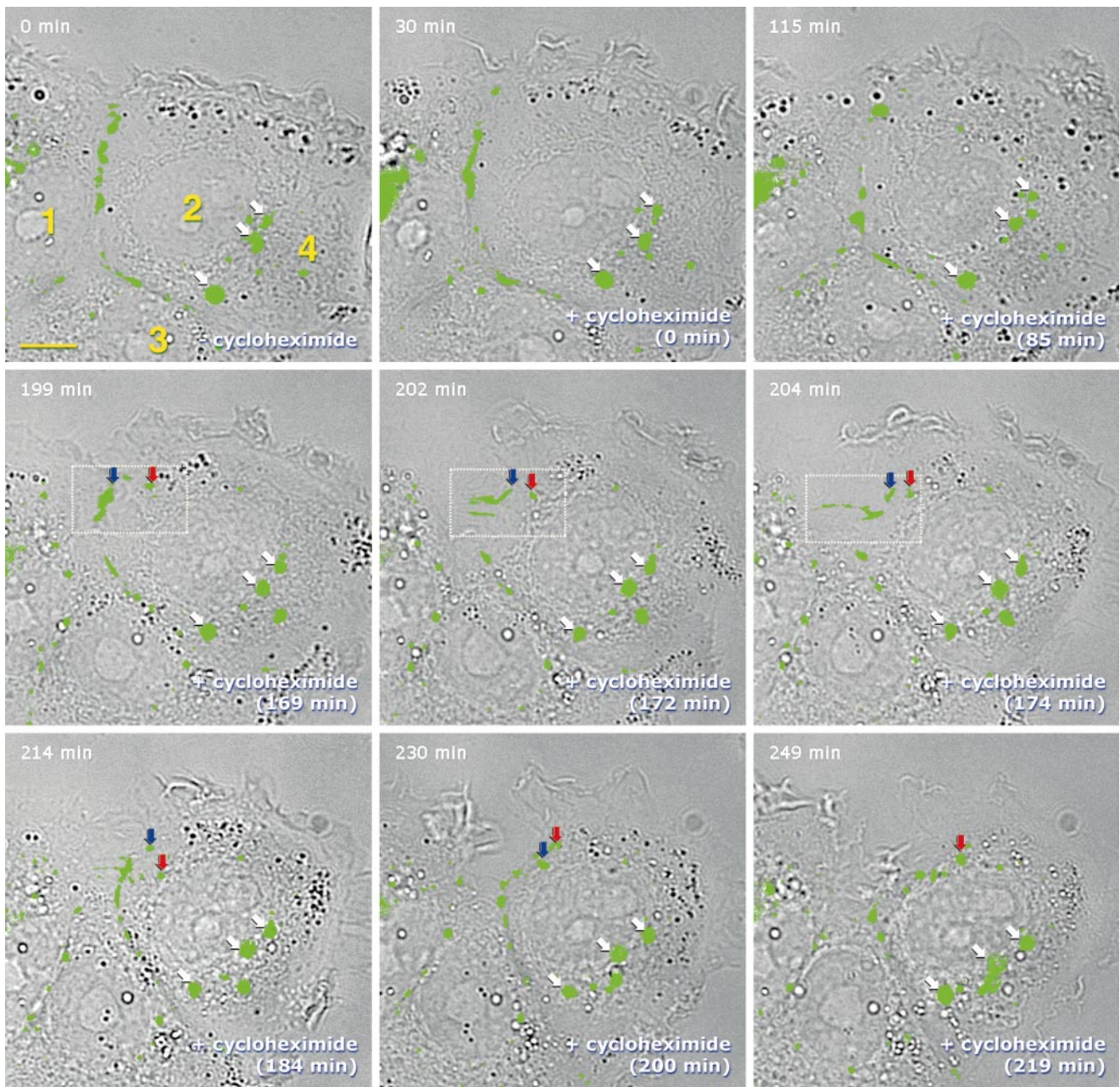


**Fig. 10** Series of overlay pictures taken from movie 5 (available at <http://www.uni-mainz.de/FB/Medizin/Anatomie/Leube/>) showing brightfield pictures merged with fluorescence pictures (green) to demonstrate Cx.EGFP-1 mobility in four PCx-9 cells before and after the addition of cycloheximide (17.1  $\mu$ M). The cells remained viable during the entire period of 249 min as judged from the ongoing undulations of peripheral cell regions (most pronounced in cell 2) and the continuous fast movements of cytoplasmic dots, which can be seen in movie 5. Note the stationary nature of large cytoplasmic vesicular structures (e.g., those labeled by white arrows in the figure) contrasting with the highly dynamic plaques at cell contact sites, which are subject to continuous remodeling. Between 199 min and 204 min, i.e., almost 3 h after the addition of cycloheximide, a large plaque is broken up (boxed area in the figure). Concurrently, cell 3 creeps between cells 1 and 2 establishing new contacts, and plaque material is taken up into cell 2 (blue and red arrow in figure). Note the overall reduction in fluorescent structures, most notably at cell contact sites between the onset and end of the experiment. Bar 10  $\mu$ m

Typically, endocytotic vesicles remained stationary and strongly fluorescent.

To determine the nature of Cx.EGFP-1-positive cytoplasmic structures further, PCx-9 cells were incubated with the fluorochrome-coupled fluid phase marker HRP. Figure 8A–A'' shows that HRP-labeled vesicles were distinct from Cx.EGFP-1-positive structures. Only sometimes was co-distribution noted in large vesicular profiles; these often contained strongly fluorescent caps of Cx.EGFP-1, indicating local clustering of chimeric connexin molecules (e.g., Fig. 8B–B'' and details in Fig. 8C–C'', D–D''). Furthermore, incubation of PCx-9 cells with fluorochrome-labeled transferrin, which is taken up by receptor-mediated endocytosis, did not result in significant labeling of Cx.EGFP-1 vesicles (Fig. 8E–E'').

Finally, to determine whether the cytoplasmic fluorescence of Cx.EGFP-1 overlaps with the lysosomal compartment, EGFP fluorescence was compared with the immunofluorescence pattern obtained with lysosomal markers (Fig. 8F–F’'). This showed that lysosomes do not colocalize with large Cx.EGFP-1 vesicles or any other Cx.EGFP-1-positive structure.

#### Gap junction reduction in cycloheximide-treated cells

It has been known for a long time that gap junctions are subject to rapid turnover given the rather short half life of their molecular subunits (Fallon and Goodenough 1981; Traub et al. 1987). To determine whether this also applies to Cx.EGFP-1-containing gap junctions, pulse-chase labeling experiments were performed by which a half life of 3.3 h was determined for the recombinant molecule (Fig. 9A), being intermediate between the value of 2.5–3 h determined for wild type connexin32 in primary hepatocytes (Traub et al. 1987) and 5 h in liver (Fallon and Goodenough 1981). On the addition of inhibitors of protein translation, one should therefore be able to follow the disassembly of gap junctions. To test this, cells were treated with cycloheximide. Figure 9B–D shows representative fluorescence micrographs of cells before the addition of cycloheximide and 4 h and 8 h afterward. At 4 h, most of the weak cytoplasmic fluorescence, especially that in close apposition to the nucleus, was no longer detectable. The number of gap junctions was also reduced. After 8 h cycloheximide treatment, the overall fluorescence was greatly reduced, and only occasional small gap junctions were visible. Remarkably, some of the large fluorescent vesicles were still present.

Next, time-lapse fluorescence microscopy was performed to follow the dynamics of gap junction reduction in cycloheximide-treated cells (Fig. 10; movie 5 at <http://www.uni-mainz.de/FB/Medizin/Anatomie/Leube/>). For movie 5, cycloheximide concentrations were chosen that were just sufficient to inhibit protein translation effectively. In order to monitor cell viability, brightfield pictures were taken just before each fluorescence image. Furthermore, after being recorded, corresponding micrograph pairs were merged into single pictures so that fluorescence patterns could be assigned directly to specific cellular regions. A threshold level was set arbitrarily above which fluorescence was scored as positive (corresponding to a green pixel), thereby extinguishing differences in fluorescence intensity and some of the weaker fluorescence. During the comparatively long recording period, hardly any fading of fluorescence occurred, and the threshold level for fluorescence detection was the same during the entire time. In movie 5, a pre-run of 30 min is first shown depicting the characteristic dynamic behavior of Cx.EGFP-1, after which cycloheximide-containing medium was pumped into the culture chamber. The addition of the drug did not visibly affect any of the typical features of gap junction dynamics. However, an overall reduction of gap junctions was noticeable with

time. Furthermore, endocytotic events appeared to be more frequent in this film (e.g., boxed area in Fig. 10) and in other recordings of cycloheximide-treated PCx-9 cells. Typically, a massive reorganization of cells and cell contacts occurred at the same time. Thus, cell 3, which was located at the bottom of the depicted area at the beginning of the observation period, slid between cells 1 and 4; this was accompanied by endocytosis and formation of new contact sites (Fig. 10, movie 5). Again, endocytosed material remained comparatively stable in the cytoplasm in vesicular form. At the end of the observation period, gap junctions and cytoplasmic vesicles were still present, although their number and the total area occupied appeared to be reduced.

#### Discussion

We have shown that a chimera consisting of a carboxy-terminally truncated version of rat connexin32 and EGFP is targeted to gap junctions of various sizes in cDNA-transfected cells. This is in agreement with several reports demonstrating that the truncation of connexin32 at the same or nearby positions does not affect trafficking, localization, or channel formation in transgenic cells (Werner et al. 1991; Levine et al. 1993; Troyanovsky et al. 1993, 1994a, 1994b; Rabadan-Diehl et al. 1994; Leube 1995; George et al. 1998, 1999), although it cannot be excluded that certain functions might be altered in vivo (cf. Rabadan-Diehl et al. 1994) or that heterologous segments interfere with function (Bruzzone et al. 1994). We do not understand why the full-length connexin32 fused to EGFP was mis-localized, but defects in channel formation and unusually strong cytoplasmic fluorescence have been reported for a comparable chimeric polypeptide consisting of full-length connexin32 and aequorin (Martin et al. 1998), and unforeseen steric hindrances may adversely affect structural and/or functional aspects of gap junction formation in these recombinant polypeptides. The highly similar pattern of autofluorescence elicited by the fusion protein Cx.EGFP-1 and the indirect immunofluorescence of antibodies directed against GFP and connexin32 further suggest that the detection of GFP fluorescence in living cells accurately reports the distribution and trafficking of the chimeric polypeptides. It should be kept in mind, however, that biosynthetic compartments might be under-represented, as fluorophore formation has been shown to occur with a considerable lag period after synthesis (Heim et al. 1994).

An important outcome of our time-lapse fluorescence microscopy of PCx-9 cells has been that gap junctional plaques are highly dynamic. By the simultaneous recording of brightfield images and fluorescence, we can exclude that these movements reflect only cell shape changes or cell motility (see, e.g., movie 5). The plaque regions are in continuous motion, moving around at considerable speed, changing shape, fusing frequently with each other, and separating into smaller patches. Lateral coalescence

and mobility of plaques have also been demonstrated for gap junctions formed by a connexin43-GFP chimera (Jordan et al. 1999). However, in contrast to Jordan et al. (1999) who were only able to record fluorescence for up to 37.3 min, we should like to stress that the gap junctions formed in our cells were highly motile. This is quite different from other junctions such as desmosomes, which we have labeled by recombinant fluorescent polypeptides in the same cell type (own unpublished observations), and other adherens junctions (Adams et al. 1998). The high degree of mobility suggests that only very little restriction is imposed by cytoskeletal elements on gap junctions. Therefore, treatment of PCx-9 cells with the microtubule-disrupting agent nocodazole or with the microfilament-disrupting drug cytochalasin does not significantly affect the dynamic behavior of fluorescent gap junctions (not shown). This is in agreement with the view that neither microfilaments nor microtubules are needed for gap junction assembly (Kidder et al. 1987; Feldman et al. 1997; George et al. 1999), although certain aspects of clustering and stability may be regulated by these filament systems (e.g., Rassat et al. 1982; Wang and Rose 1995), and connexins may associate with cortical linker and/or signaling molecules (e.g., Giepmans and Moolenaar 1998; Toyofuku et al. 1998).

In addition to the mobility of entire gap junctional plaques within the plasma membrane, we have also observed dynamic heterogeneities within plaques. These differences in fluorescence intensity can be attributed to the superimposition of fluorescent vesicles in close vicinity of Cx.EGFP-1-positive plaques and to localized membrane infoldings. Alternatively, they could reflect different packing densities of membrane particles in the junctional macula. Whether such heterogeneities, which have been known for a long time, are of relevance for channel function is not clear (cf. Johnson et al. 1989; Goodenough et al. 1996). However, along these lines, it should be of interest to determine whether these subdomains correlate to specific connexon groups that are either in the process of entering or leaving plaque regions (Johnson et al. 1989) and which factors influence their formation and mobility.

The investigation of the biosynthesis of the gap junction is complicated, in our system, by the finding that the synthesis of GFP and initiation of fluorescence probably do not coincide (see, e.g., Heim et al. 1994). Since mature gap junctions are formed, we conclude however that Cx.EGFP-1 passes the "quality control" step in the ER (for ER retention of mutants see, e.g., Leube 1995) and assume that it is transported through the secretory pathway. This notion is also supported by observations involving the use of comparable connexin32-aequorin chimeras localized to ER and Golgi compartments (George et al. 1999). Since clear exocytotic fusion events of larger vesicles are not detectable in our films, we suspect that some of the multiple and weakly fluorescent vesicles moving at high speed connect the biosynthetic compartments with each other and the plasma membrane. Accordingly, these compartments are reduced when cells are treated with cycloheximide. Therefore, gap junctions are probably

formed from Cx.EGFP-1 at the cell surface by the apposition of oligomers that are provided in small vesicles and not by the addition of large pre-assembled clusters. This fits the concept of gap junction formation, whereby oligomerization occurs gradually along the exocytotic route in the ER and Golgi compartments (Musil and Goodenough 1993; Puranam et al. 1993; Rahman et al. 1993; Kumar et al. 1995; Laird et al. 1995; Leube 1995; George et al. 1999) and gap junction assembly takes place at the cell surface by the recruitment of small aggregates (Benedetti et al. 1974; Johnson et al. 1974, 1989). Experiments are under way in which our cells are treated with drugs with the aim of enriching transport intermediates in specific compartments (see, e.g., Musil and Goodenough 1993; Laird et al. 1995; Wang and Rose 1995; Feldman et al. 1997) at a level sufficient for clear visualization to follow further trafficking after release of the block in quasi pulse-chase experiments in living cells (compare with Wacker et al. 1997; Hirschberg et al. 1998).

Efficient mechanisms must exist to remove connexin molecules given the short half life that has been determined in this study and that is similar to the half life determined for wild type connexin32 *in vivo* and in primary culture (Fallon and Goodenough 1981; Traub et al. 1987). Two principal modes can be envisaged. Either complete junctional plaques are removed by endocytosis, and connexin molecules are subsequently degraded or reutilized. Alternatively, small subunits are removed from the plaques either by dispersal or by endocytosis and are subjected to degradation or reutilization.

The occurrence of annular gap junctions in the cytoplasm has been taken as evidence for the endocytosis of large gap junctional plaques encompassing plasma membranes from both abutting cells (Larsen and Risinger 1985; Sasaki and Garant 1986; Laird 1996). We have documented endocytotic events that could represent this process in Figs. 7 and 10 and the corresponding movies 3–5, whereby long tubular structures are formed that eventually pinch off. In agreement with the rare occurrence of these events, only a very few cytoplasmic connexin32-EGFP vesicles could be labeled with the fluid phase marker HRP and even fewer with the receptor-specific endocytosis marker transferrin (compare also with the lack of co-distribution of transferrin receptor and a connexin32 chimera in Leube 1995). Remarkably, fluorescence in endocytosed vesicles remains stable for considerable periods of time. Therefore, it is no surprise that cytoplasmic Cx.EGFP-1 only rarely co-localizes with lysosomal polypeptides (see also Leube 1995), although this is in contrast to previous observations by others suggesting the lysosomal degradation of cytoplasmic gap junctions (e.g., Larsen and Hainan 1978; Sasaki and Garant 1986; Gregory and Bennett 1988; Rahman et al. 1993). We conclude that endocytosis of gap junctions and lysosomal degradation do not account alone for the high turnover of gap junctions and their connexin molecules in our cells; future experiments will have to show whether the importance of annular gap junctions as a regulatory compartment for gap junction dynamics has been overemphasized in the past.

The removal of gap junctions also appears to be regulated in a way that is difficult to visualize. Whereas it is comparatively easy to detect closely clustered molecules in plaques, it is much more difficult to identify small oligomers or even single connexin molecules unambiguously. Therefore, small vesicles or membrane regions carrying only a few connexin molecules may be barely above the detection limit of fluorescence microscopy. Potential candidate carriers are the multiple small and rapidly moving puncta that we have seen in all movies but that are just above background and difficult to follow between frames. These structures do not only shuttle between biosynthetic compartments as suggested by observations in cycloheximide-treated cells that did not completely lose these flickering puncta (not shown).

In an attempt preferentially to detect modes of gap junction disassembly, cells were treated with the translation inhibitor cycloheximide. It should be noted, however, that connexin molecules synthesized before the addition of the drug continue to be integrated into gap junctions (Laird et al. 1995). We therefore consider that the initial reduction of cytoplasmic fluorescence in cycloheximide-treated cells is a result of the depletion of biosynthetic and secretory compartments. Clearly, gap junction assembly is also not inhibited after cycloheximide addition, as we have noted new contact formation between rearranged cells in accordance with reports by others (Epstein et al. 1977; Tadvalkar and Da Silva 1983). Interestingly, increased cell motility and elevated rates of endocytosis are often observed in our cycloheximide-treated cells. This could be the consequence of an overall reduction of cell adhesiveness because of drug-induced destabilizing effects on other cell-to-cell junctions whose dynamics have been shown to be linked to gap junction morphogenesis (e.g., Fujimoto et al. 1997; Wang and Rose 1997). The continuous loss of junctional and vesicular fluorescence in cycloheximide-treated cells suggests that, similar to assembly, the disassembly of gap junctions is a dynamic process involving gradual subunit removal.

In conclusion, we have established and characterized cell lines that can be used as model systems to examine gap junctions in living cells. We have shown that gap junctions are highly motile structures that can be monitored for many hours under defined culture conditions, thereby enabling the investigation of mechanisms that determine gap junction formation and disassembly in single cells. Our results suggest that gap junction morphogenesis is regulated at the subunit level probably involving small and rapidly moving vesicles (compare also with Jordan et al. 1999) and by endocytosis of gap junctional fragments into a non-lysosomal compartment.

**Acknowledgements** The authors thank Dr. V. Krutovskikh (International Agency for Research on Cancer, Lyon, France) for the generous gift of connexin antibodies. Monoclonal antibody H4B4 was obtained from the Developmental Studies Hybridoma Bank maintained by the Department of Biology at the University of Iowa, Iowa City, Iowa, USA, under contract number N01-HD-2-3144 from the NICHD.

## References

- Adams CL, Chen Y-T, Smith SJ, Nelson WJ (1998) Mechanisms of epithelial cell-cell adhesion and cell compaction revealed by high-resolution tracking of E-cadherin-green fluorescent protein. *J Cell Biol* 142:1105–1119
- Benedetti EL, Dunia I, Bloemendal H (1974) Development of junctions during differentiation of lens fibers. *Proc Natl Acad Sci USA* 71:5073–5077
- Bruzzone R, White TW, Paul DL (1994) Expression of chimeric connexins reveals new properties of the formation and gating behavior of gap junction channels. *J Cell Sci* 107:955–967
- Bruzzone R, White TW, Paul DL (1996) Connections with connexins: the molecular basis of direct intercellular signaling. *Eur J Biochem* 238:1–27
- Dahl G, Miller T, Paul D, Voellmy R, Werner R (1987) Expression of functional cell-cell channels from cloned rat liver gap junction complementary DNA. *Science* 236:1290–1292
- Donaldson P, Eckert R, Green C, Kistler J (1997) Gap junction channels: new roles in disease. *Histol Histopathol* 12:219–231
- Eghbali B, Kessler JA, Spray DC (1990) Expression of gap junction channels in communication-incompetent cells after stable transfection with cDNA encoding connexin 32. *Proc Natl Acad Sci USA* 87:1328–1331
- Elfgang C, Eckert R, Lichtenberg-Fraté H, Butterweck A, Traub O, Klein RA, Hülser DF, Willecke K (1995) Specific permeability and selective formation of gap junction channels in connexin-transfected HeLa cells. *J Cell Biol* 129:805–817
- Elvira M, Diez JA, Wang KKW, Villalobo A (1993) Phosphorylation of connexin-32 by protein kinase C prevents its proteolysis by  $\mu$ -calpain and m-calpain. *J Biol Chem* 268:14294–14300
- Epstein ML, Sheridan JD, Johnson RG (1977) Formation of low-resistance junctions in vitro in the absence of protein synthesis and ATP production. *Exp Cell Res* 104:25–30
- Falk MM, Kumar NM, Gilula NB (1994) Membrane insertion of gap junction connexins: polytopic channel forming membrane proteins. *J Cell Biol* 127:343–355
- Fallon RF, Goodenough D (1981) Five-hour half-life of mouse liver gap-junction protein. *J Cell Biol* 90:521–526
- Feldman PA, Kim J, Laird DW (1997) Loss of gap junction plaques and inhibition of intercellular communication in ilimaquinone-treated BICR-M1R<sub>k</sub> and NRK cells. *J Membr Biol* 155:275–287
- Fujimoto K, Nagafuchi A, Tsukita S, Kuraoka A, Ohokuma A, Shibata Y (1997) Dynamics of connexins, E-cadherin and  $\alpha$ -catenin on cell membranes during gap junction formation. *J Cell Sci* 110:311–322
- George CH, Kendall JM, Campbell AK, Evans WH (1998) Connexin-aequorin chimerae report cytoplasmic calcium environments along trafficking pathways leading to gap junction biogenesis in living COS-7 cells. *J Biol Chem* 273:29822–29829
- George CH, Kendall JM, Evans WH (1999) Intracellular trafficking pathways in the assembly of connexins into gap junctions. *J Biol Chem* 274:8678–8685
- Giepmans BNG, Moolenaar WH (1998) The gap junction protein connexin43 interacts with the second PDZ domain of the zona occludens-1 protein. *Curr Biol* 8:931–934
- Goodenough DA, Revel JP (1970) A fine structural analysis of intercellular junctions in the mouse liver. *J Cell Biol* 45:272–290
- Goodenough DA, Goliger JA, Paul DL (1996) Connexins, connexons, and intercellular communication. *Annu Rev Biochem* 65:475–502
- Gregory WA, Bennett MVL (1988) Gap junctions in goldfish retinal ependyma: regional variation in cellular differentiation. *Dev Brain Res* 42:205–216
- Heim R, Prasher DC, Tsien RY (1994) Wavelength mutations and posttranslational autooxidation of green fluorescent protein. *Proc Natl Acad Sci USA* 91:12501–12504
- Hirschberg K, Miller CM, Ellenberg J, Presley JF, Siggia ED, Phair RD, Lippincott-Schwartz J (1998) Kinetic analysis of secretory protein traffic and characterization of Golgi to plasma

- membrane transport intermediates in living cells. *J Cell Biol* 143:1485–1503
- Johnson R, Hammer M, Sheridan J, Revel J-P (1974) Gap junction formation between reaggregated Novikoff hepatoma cells. *Proc Natl Acad Sci USA* 71:4536–4540
- Johnson RG, Meyer RA, Lampe PD (1989) Gap junction formation: a “self-assembly” model involving membrane domains of lipid and protein. In: Sperelakis N, Cole WC (eds) *Cell interactions and gap junctions*. CRC Press, Boca Raton, pp 159–179
- Jordan K, Solan JL, Dominguez M, Sia M, Hand A, Lampe PD, Laird DW (1999) Trafficking, assembly, and function of a connexin43-green fluorescent protein chimera in live mammalian cells. *Mol Biol Cell* 10:2033–2050
- Kidder GM, Rains J, McKeon J (1987) Gap junction assembly in the preimplantation mouse conceptus is independent of microtubules, microfilaments, cell flattening, and cytokinesis. *Proc Natl Acad Sci USA* 84:3718–3722
- Koval M, Harley JE, Hick E, Steinberg TH (1997) Connexin46 is retained as monomers in a *trans*-Golgi compartment of osteoblastic cells. *J Cell Biol* 137:847–857
- Krutovskikh V, Yamasaki H (1997) The role of gap junctional intercellular communication (GJIC) disorders in experimental and human carcinogenesis. *Histol Histopathol* 12:761–768
- Krutovskikh V, Mazzoleni G, Mironov N, Omori Y, Aguelon A-M, Mesnil M, Berger F, Partensky C, Yamasaki H (1994) Altered homologous and heterologous gap-junctional intercellular communication in primary human liver tumors associated with aberrant protein localization but not gene mutation of connexin 32. *Int J Cancer* 56:87–94
- Kumar NM, Gilula NB (1996) The gap junction communication channel. *Cell* 84:381–388
- Kumar NM, Friend DS, Gilula NB (1995) Synthesis and assembly of human  $\beta_1$  gap junctions in BHK cells by DNA transfection with the human  $\beta_1$  cDNA. *J Cell Sci* 108:3725–3734
- Laing JG, Beyer EC (1995) The gap junction protein connexin43 is degraded via the ubiquitin proteasome pathway. *J Biol Chem* 270:26399–26403
- Laing JG, Tadros PN, Westphale EM, Beyer EC (1997) Degradation of connexin43 gap junctions involves both the proteasome and the lysosome. *Exp Cell Res* 236:482–492
- Laird DW (1996) The life cycle of a connexin: gap junction formation, removal and degradation. *J Bioenerg Biomembr* 28:311–318
- Laird DW, Castillo M, Kasprzak L (1995) Gap junction turnover, intracellular trafficking, and phosphorylation of connexin43 in brefeldin A-treated rat mammary tumor cells. *J Cell Biol* 131:1193–1203
- Lane NJ, Swales LS (1980) Dispersal of junctional particles, not internalization, during the in vivo disappearance of gap junctions. *Cell* 19:579–586
- Larsen WJ, Hai-Nan (1978) Origin and fate of cytoplasmic gap junctional vesicles in rabbit granulosa cells. *Tissue Cell* 10:585–598
- Larsen WJ, Risinger MA (1985) The dynamic life histories of intercellular membrane junctions. *Mod Cell Biol* 4:151–216
- Leube RE (1995) The topogenic fate of the polytopic transmembrane proteins, synaptophysin and connexin, is determined by their membrane-spanning domains. *J Cell Sci* 108:883–894
- Levine E, Werner R, Neuhaus I, Dahl G (1993) Asymmetry of gap junction formation along the animal-vegetal axis of *Xenopus* oocytes. *Dev Biol* 156:490–499
- Martin PEM, George CH, Castro C, Kendall JM, Capel J, Campbell AK, Revilla A, Barrio LC, Evans WH (1998) Assembly of chimeric connexin-aequorin proteins into functional gap junction channels. *J Biol Chem* 273:1719–1726
- Musil LS, Goodenough DA (1991) Biochemical analysis of connexin43 intracellular transport, phosphorylation, and assembly into gap junctional plaques. *J Cell Biol* 115:1357–1374
- Musil LS, Goodenough DA (1993) Multisubunit assembly of an integral plasma membrane channel protein, gap junction connexin43, occurs after exit from the ER. *Cell* 74:1065–1077
- Naus CCG, Hearn S, Zhu D, Nicholson BJ, Shivers RR (1993) Ultrastructural analysis of gap junctions in C6 glioma cells transfected with connexin43 cDNA. *Exp Cell Res* 206:72–84
- Oyamada M, Kimura H, Oyamada Y, Miyamoto A, Ohshika H, Mori M (1994) The expression, phosphorylation, and localization of connexin 43 and gap-junctional intercellular communication during the establishment of a synchronized contraction of cultured neonatal rat cardiac myocytes. *Exp Cell Res* 212:351–358
- Puranam KL, Laird DW, Revel J-P (1993) Trapping an intermediate form of connexin43 in the Golgi. *Exp Cell Res* 206:85–92
- Rabadan-Diehl C, Dahl G, Werner R (1994) A connexin-32 mutation associated with Charcot-Marie-Tooth disease does not affect channel formation in oocytes. *FEBS Lett* 351:90–94
- Rahman S, Carlile G, Evans WH (1993) Assembly of hepatic gap junctions. Topography and distribution of connexin 32 in intracellular and plasma membranes determined using sequence-specific antibodies. *J Biol Chem* 268:1260–1265
- Rassat J, Robenek H, Themann H (1982) Alterations of tight and gap junctions in mouse hepatocytes following administration of colchicine. *Cell Tissue Res* 223:187–200
- Sasaki T, Garant PR (1986) Fate of annular gap junctions in the papillary cells of the enamel organ in the rat incisor. *Cell Tissue Res* 246:523–530
- Severs NJ, Shovel KS, Slade AM, Powell T, Twist VW, Green CR (1989) Fate of gap junctions in isolated adult mammalian cardiomyocytes. *Circ Res* 65:22–42
- Simon AM, Goodenough DA (1998) Diverse functions of vertebrate gap junctions. *Trends Cell Biol* 8:477–483
- Swenson KI, Jordan JR, Beyer EC, Paul DL (1989) Formation of gap junctions by expression of connexins in *Xenopus* oocyte pairs. *Cell* 57:145–155
- Tadvalkar G, Da Silva PP (1983) In vitro, rapid assembly of gap junctions is induced by cytoskeleton disruptors. *J Cell Biol* 96:1279–1287
- Toyofuku T, Yabuki M, Otsu K, Kuzuya T, Hori M, Tada M (1998) Direct association of the gap junction protein connexin-43 with ZO-1 in cardiac myocytes. *J Biol Chem* 273:12725–12731
- Traub O, Look J, Paul D, Willecke K (1987) Cyclic adenosine monophosphate stimulates biosynthesis and phosphorylation of the 26 kDa gap junction protein in cultured mouse hepatocytes. *Eur J Cell Biol* 43:48–54
- Troyanovsky SM, Eshkind LG, Troyanovsky RB, Leube RE, Franke WW (1993) Contributions of cytoplasmic domains of desmosomal cadherins to desmosome assembly and intermediate filament anchorage. *Cell* 72:561–574
- Troyanovsky SM, Troyanovsky RB, Eshkind LG, Krutovskikh VA, Leube RE, Franke WW (1994a) Identification of the plakoglobin-binding domain in desmoglein and its role in plaque assembly and intermediate filament anchorage. *J Cell Biol* 127:151–160
- Troyanovsky SM, Troyanovsky RB, Eshkind LG, Leube RE, Franke WW (1994b) Identification of amino acid sequence motifs in desmocollin, a desmosomal glycoprotein, that are required for plakoglobin binding and plaque formation. *Proc Natl Acad Sci USA* 91:10790–10794
- Wacker I, Kaether C, Krömer A, Migala A, Almers W, Gerdes HH (1997) Microtubule-dependent transport of secretory vesicles visualized in real time with a GFP-tagged secretory protein. *J Cell Sci* 110:1453–1463
- Wang Y, Rose B (1995) Clustering of Cx43 cell-to-cell channels into gap junction plaques: regulation by cAMP and microfilaments. *J Cell Sci* 108:3501–3508
- Wang Y, Rose B (1997) An inhibition of gap-junctional communication by cadherins. *J Cell Sci* 110:301–309
- Werner R, Levine E, Rabadan-Diehl C, Dahl G (1989) Formation of hybrid cell-cell channels. *Proc Natl Acad Sci USA* 86:5380–5384
- Werner R, Levine E, Rabadan-Diehl C, Dahl G (1991) Gating properties of connexin32 cell-cell channels and their mutants expressed in *Xenopus* oocytes. *Proc R Soc Lond [Biol]* 243:5–11
- Windoffer R, Borchert-Stuhlträger M, Haass NK, Thomas S, Hergt M, Bulitta CJ, Leube RE (1999) Tissue expression of the vesicle protein pantophysin. *Cell Tissue Res* 296:499–510